Superhard Nanocomposite and Nanostructural Ti-Si-B-N Coatings

Yu.P. Pinzhin, S.V. Ovchinnikov, A.N. Tyumentsev, A.D. Korotaev*, V.Yu. Moshkov*, V.M. Savostikov**ϭ D.P. Borisov**

Institute of Strength Physics and Materials Science SB RAS, Akademicheski 2/1, Tomsk, 634021, Russia, phone (3822)531569, pinzhin@phys.tsu.ru
**Tomsk State University, 36 Lenin Prospekt, Tomsk, 634050, Russia*
*** Technotron State Organization, 33 Visotski st., Tomsk,634031, Russia*

Abstract – The dependence of changes in strength properties of nanocomposite Ti-Si-B-N coatings with high content of oxygen and carbon impurities on a fine structure was studied using electron microscopy and measuring micro- and nanohardness. A two-level grain structure is shown to form under conditions of low temperature deposition (T=200 °C). The structure is characterized by fragmentation of 0.1–0.2 μm grains into 15–20 nm subgrains with pronounced texture. The coatings with the grain size <15 nm and high amorphous component are produced as the content of silicon increases. At deposition temperatures 400–450 °C, a nanocomposite structure is observed whose grain size is 10–15 nm, no texture in the structure being seen. The hardness (H_μ) is measured to be >40–50 GPa at optimum compositions and conditions of synthesis. It can be assumed that superhardness will be achieved with multi-phase grain-boundary interlayers >1 nm.

1. Introduction

Within the past 10 years a number of superhard (H_μ>40 GPa) and ultrahard (H_μ=80÷100 GPa) [1–3] nanocomposite n-MeN/a-phase-type coatings (n-MeN – nanocrystal nitrides of transition metals Ti, Zr, Ta, W, a-phase – amorphous phase SiN_x, BN, TiB_2) have been developed. During deposition, there occurs thermodynamically-induced phase separation to form nanocrystal nitrides and amorphous phases insoluble in them at T<(1100÷1200) °C. The latter segregate at nanocrystal boundaries and inhibit grain growth. The nanocomposite structure and superhardness of this coatings are thermally stable up to T=1100 °C [4, 5].

The hardness H_μ>40 Gpa and its reliable reproducibility can be achieved provided certain deposition conditions are fulfilled (temperature interval, optimal silicon content, and partial nitrogen pressure sufficient for formation of a number of amorphous phases corresponding to the percolation threshold, minimum impurity concentration, etc.) [3–5].

According to [3, 4, 6], the nanosize of nitride crystals and the presence of a fine interlayer (<1 nm) of amorphous phase with highly strong interatomic bond with the crystal-phase atoms are the factors responsible for superhardness in nanocomposites. First, this suppresses dislocation plasticity, second, makes an effective hindrance to nucleating microcrack propagation, and, third, renders grain-boundary sliding impossible.

Superhardness (H_μ=40÷50 GPa) was also achieved in TiN-Cu, ZrN-Ni, and ZrN-Y coatings, where a metallic phase is segregated at the nitride nanocrystallite [4,7]. However, the maximum values of H_μ for these coatings are found at d=20÷30 nm, that is, on realization of dislocation plasticity, and the hardness decreases down to 20÷25 GPa either at relatively low annealing temperatures (T<600÷650 °C) [4,8] or at long times of aging at room temperature [4].

High internal compression stresses are found in all coatings with low thermal stability of superhardness, the coatings being deposited under irradiation of ions whose energy is higher than the threshold bias energy. Due to this fact, superhardness is associated with the synergetic effect of small grain sizes, high internal stresses, and radiative defects [4, 8].

It is noted in [4, 9] that internal stresses are of great importance. Yet, hardness values prove to be close in the Ti-Si-N and Ti-B-N coatings deposited by magnetron sputtering, where compression stresses appear to be extremely high (up to 10 GPa) [10] and in the Ti-Si-N coatings deposited by PCVD where internal stresses are insignificant [11].

A fine defect structure of nanocrystallites, the presence of impurities, and their complexes with lattice defects can be the most important factors for superhardness to be achieved. Unfortunately, the defect substructure in nanocrystal states is still not understood due to the problems of its experimental examination. It is noted in [12], that a subgrain structure is likely to exist in the TiN coatings with a grain size of d=20÷25 nm, however, the attempts to investigate into it failed. Of special interest are the experimental data characterizing the states of defect structures in nanocomposite coatings.

We have developed a special technique [13] of electron microscope analysis of misorientations of crystalline lattice which allows us to quantify the elastic-plastic tensor components of curvature-torsion of the lattice with assessment of local internal stresses. In this work, we have studied some features of phase-structure states and defect substructure of nanocrystal Ti-Si-B-N coatings of varying composition using the foregoing method.

2. Experimental technique

The coatings were deposited by magnetron sputtering simultaneously from two cathodes and plasma generator of nitrogen ions. One of the cathodes was a compound of titanium, silicon, and boron in equal proportions, whereas the second one – titanium of 99.7 %. The titanium content was varied by adjusting cathode currents (Table 1). Use was made of the $Ar+N_2$ mixture at the partial nitrogen pressure ~ 0.04 Pa.

Table 1. Deposition regimes for coatings and their microhardness

No.	Cathode current relation Ti/Ti-Si-B; deposition temperature	Mean hardness H_μ, GPa
1	1/1; T = 200 °C	21÷24
2	3/1; T =200 °C	33÷34
3	4.5/1; T =200 °C	43÷46
4	5.6/1; T =200 °C	43÷46
5	5.6/1; T = 400–450 °C	50÷55

3. Experimental results

A microdiffraction pattern testifying to the preferred orientation of coating nanocrystals with respect to substrate grains (Fig. 1, *a*) is revealed for a thin layer (h<150 nm) adjacent to the substrate in coatings 4 (Table 1). The crystallite size in the coating is found to be 20÷25 nm (Fig. 1, *b*). In so doing, we observed only those reflections which correspond to titanium nitride TiN with the lattice constant a=(0.421±0.001) nm.

A growth texture <200> is developed with increase in the coating thickness as evidenced by the absence of diffraction ring (111) in the microelectron diffraction patterns (Fig. 2, *a*). A characteristic feature of contrast is the presence of a large number of multiple narrow extinction contours (Fig. 2, *b*) which continuously move as the foil in the microscope column is tilted, and this is typical of the structures with a high curvature of crystal lattice [13]. In this case, the grain size can be measured from the extinction-contour motion in the dark field as the specimen is tilted in the microscope column. The grain size was measured to be 0.1÷0.2 μm.

Notably, a speckled contrast (Fig. 3) is revealed in the dark-field images of extinction contours. A regular change in the contrast with the specimen tilt suggests the presence of grain-boundary angles between the corresponding regions in the crystal. The angles were estimated to be <5°.

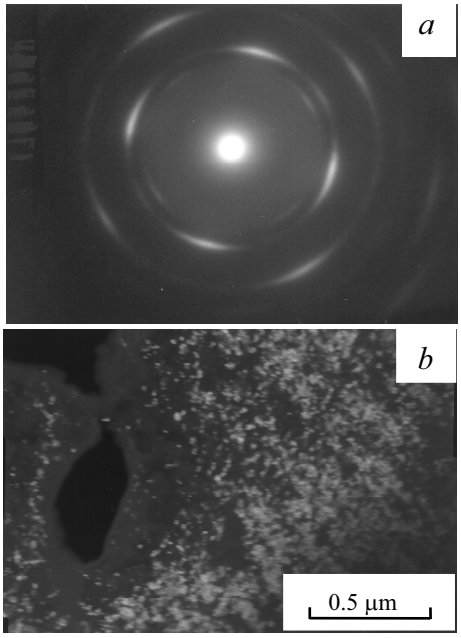

Fig. 1. Diffraction pattern (a) and dark field image (b) of TiN-Si-B (No 3, tab. 1) coating near coating-substrate interface

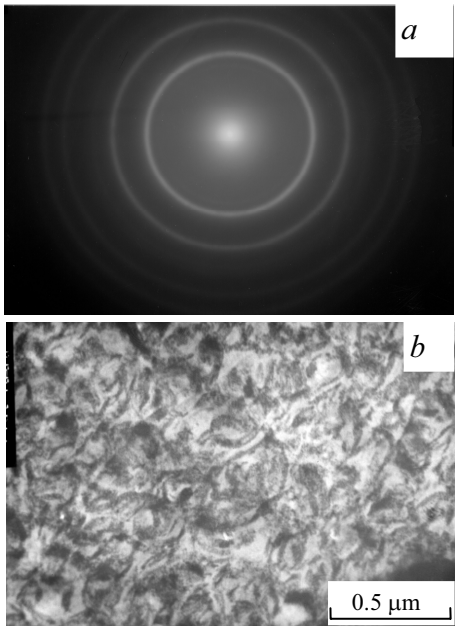

Fig. 2. Diffraction pattern (a) and bright field image (b) of TiN-Si-B (No 3, tab. 1) coating on 1 μm from coating-substrate interface

Thus, the TiN microcrystallites in the coatings under study possess a two-level structure. The fragmentation leads to continuous rings in microelectron diffraction patterns (Fig. 2, *a*) instead of reflections from individual grains observed in the case where the grain size d=0.1÷0.2 μm.

The two-level structure makes the most volume of the coating. In addition, one can observe regions with the nanocrystalline structure whose grain size is 10÷15 nm.

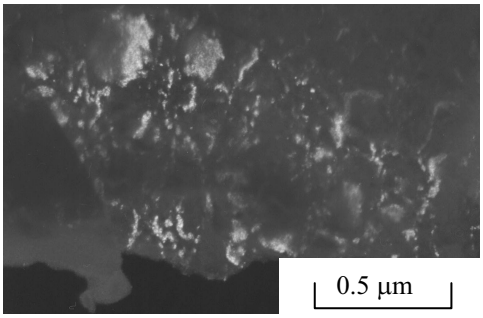

Fig. 3. Dark field image of TiN-Si-B (No 3, tab.1) coating

The revealed inhomogeneity was assumed to point to incompletion of phase separation in the multielement system under investigation at a relatively low (T=200 °C) synthesis temperatures of coating. In this connection, the structure of phase separations was examined at elevated synthesis temperatures 400÷450 °C. It was found that the proportion of the two-level structure is significantly decreased, and such a coating is largely a nanostructure with the grain size d=10÷15 nm (Fig. 4, *b*). No texture was observed in this case (Fig. 4, *a*).

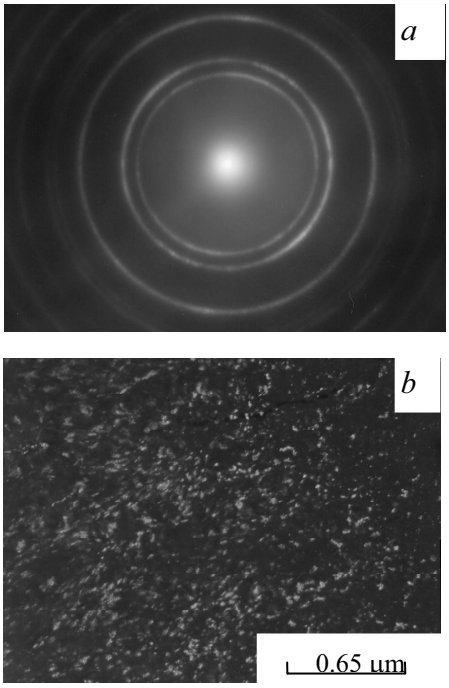

Fig. 4. Diffraction pattern (a) and bright field image (b) of TiN-Si-B (No 5, tab. 1) coating on 1 m from coating-substrate interface

Coating structure is essentially changed throughout the thickness with increase in the silicon content. A nanocrystalline structure with random TiN crystallite (d=10 nm) orientation is seen in the region where the coating is adjacent to the substrate. The structure remains nanocrystalline as the coating thickness is increased, and no increase in the grain size is found (Fig. 5, *b*). The ring widths (200) and (220) (Fig. 5, *a*) are markedly increased, which is due to the decrease in crystallite size. In the microelecron diffraction pattern, one can clearly see an increased diffuse-scattering background (Fig. 5, *a*), which suggests a significant volume fraction of an amorphous component in the structure. Moreover, fairly extensive regions are manifested where such a considerable broadening of diffraction rings and high diffuse-scattering background are revealed that the structure should probably be qualified as an amorphous-crystalline one.

As the titanium concentration is increased as compared with the alloying components in the coatings, their hardness H_μ considerably increases and achieves the values typical of superhard coatings (Table 1). The values of H_μ listed in the table were obtained at P=200 mN, where the indentation depth was about half the coating thickness. In this case, the measured hardness corresponds to the hardness of the substrate-coating composition due to plastic deformation of the substrate. In this connection, nanohardness was measured at the indenter loads 20 mN and 8 mN. Figure 6 shows several loading-unloading curves as examples. At 20 mN, H_μ appears to be close to those given in Table 1, whereas the hardness values essentially exceed those as the load is decreased down to 8 mN. For example, coating 4 (table 1) has the hardness $H_\mu \cong$70 Gpa at a load of 8 mN.

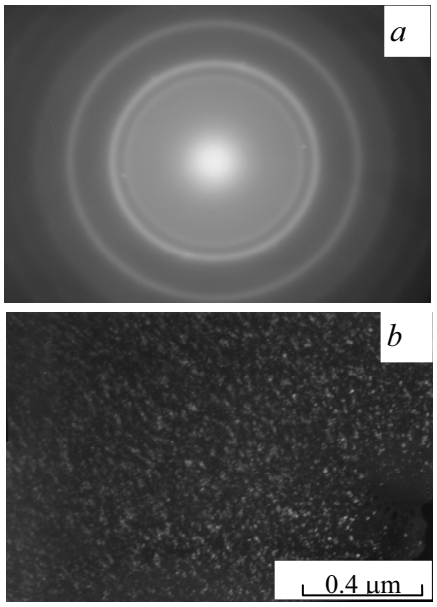

Fig. 5. Diffraction pattern (a) and bright field image (b) of TiN-Si-B (No 2, tab. 1) coating

It was pointed out above that the microstructure changes from a two-level grain one to a nanocrystalline with increase in the synthesis temperature of coatings from 200 up to 400÷450 °C. Obviously, the separation of phases involved must be more complete in this case. The hardness values measured at P=200 mN were also found to be essentially higher than those obtained upon deposition of coatings at 200 °C (Table 1). Thus, su-

perhard Ti-Si-B-N coatings with high contents of oxygen and carbon impurities can be produced by optimizing compositions and deposition conditions.

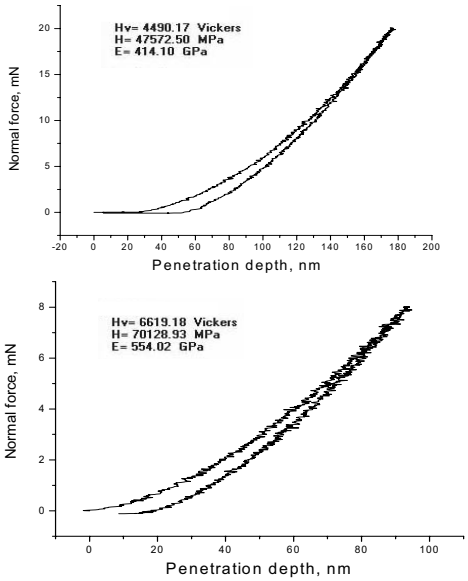

Fig. 6. Nanohardness test of TiN-Si-B (No 4, tab. 1) coating

4. Discussion

The presence of a two-level grain structure is one of the most interesting features of coating microstructure resulting under low-temperature deposition (T=200 °C). In so doing, regular misorientation of nanosized subgrains is revealed which is similar to that observed under polygonization of bend crystals. It should also be noted that the axial structure (200) is observed in the presence of the two-level grain structure, and grain size values measured from X-ray line broadening by X-ray diffraction analysis are found to be close to those of fragments (15÷20) nm with low grain-boundary angles (Fig. 3).

It is well known that the grain size found by X-ray diffraction is (20÷25) nm for very much pronounced texture (111) of the ZrN/Cu coatings [14] and texture (200) for the ZrN/Y coatings [7]. It can be assumed that in fact these values correspond to the regions of coherent scattering of crystals in a columnar structure. The cross-sections of the crystals far exceed the foregoing grain size. This assumption is supported by the presence of strong texture. Indeed, it seems unlikely that on the surface of a growing coating there occurs continuous nucleation of preferred-oriented grains.

We believe that the texturized n-MeN/ metal or n-MeN/a-phase coatings must have a two-level grain structure, similar to that found in this work, with submicrocrystalline (d=0.1÷0.3 μm) in the cross-sections of columnar crystals subject to fragmentation into the nanosize subgrains d=25÷30 nm with low grain-boundary angles. The fragmentation appears to result from polygonization of highly defective elastically-strained columnar crystals. The low-angle boundaries are known to be made of individual dislocations, therefore at these boundaries there is no preferred formation of layers of a grain-boundary phase suppressing grain growth. This may be assumed to result in a low thermal stability of superhardess states for n-MeN/metal coatings due to relaxation of the defect substructure at relatively low temperatures (T<700 °C)

Thus, superhard coatings with columnar structure have low thermal stability and are not in essence nanocomposite coatings. In this context, the coatings with two-level structure we deposited at low-temperature synthesis are not nanocomposite and must have a low temperature of superhardness degradation.

It was emphasized in [4,11,2] that neither columnar structure nor texture are observed in superhard nanocomposite coatings deposited under synthesis conditions optimal for phase separation.

In accordance with the foregoing, the coatings deposited at T=400÷450 °C can be considered as nanocomposite ones, though their grain size d = 15 20 nm far exceeds that typical of superhard nanocomposite coatings (d=3÷8 nm) [4, 10]. In [2, 11], superhardness in the nanocomposite n-TiN/a-BN coatings was also achieved at the grain size d = 20 25 nm. This gives grounds to expect that the presence of a fine grain-boundary interlayer (Δh<1 nm) is not critical for achieving superhardness.

We believe that superhardness can be achieved at a fairly high hardness of grain-boundary phases. In addition to this factor, the presence of many phases in the grain-boundary layer separating nanocrystallites seems to be of a critical importance. Obviously, the latter, resulting in the complexity of accommodation of nucleating-crack propagation, the changes in the dislocation Burgers vectors and sliding systems at the phase boundaries must increase adhesive strength of nanocomposite boundaries. This leads us to suggest that it is multielement systems that must be promising for deposition of superhard nanocomposite coatings, since mutually insoluble amorphous nanocrystalline grain-boundary phases are formed in such systems under synthesis. The presence of boron, oxygen, carbon, nitrogen, and silicon in the composition of the coatings studied seems to lead to formation, in addition to nanocrystalline $Ti_{1-x}Si_xN$, of amorphous, or amorphous-crystalline phases similar to borides, carbides, and oxides. These phases possess high interatomic bonds and hardness. Therefore, superhardness is observed even in the case where the grain-boundary thickness exceeds 1 nm.

The work was supported by RFBR grant No 05-08-01277 and BRHE program (project No 016-02).

References

1. D.G. Morris *Material Science, Foundation*, vol. 2 Trans. Tech. Publication LVD Switzerland, Germany, UK, USA 1998, p. 1–84.

2. P. Kavrankova, M.G.J. Veprek-Heijman, O. Zindulka, A. Bergmaeir, S. Veprek, Surf. Coat. Technol. 163–164, 149 (2003).
3. S. Veprek J., Vac. Sci. Technol. A 17, 2401 (1999).
4. S. Veprek, M.G.J. Veprek-Heijman, P. Kavrankova, J. Prohazka, Thin Solid Films 476, 1 (2005).
5. H.D. Manuling, D.S. Patil, K. Moto, M. Jilek, S. Veprek, Surf. Coat. Technol. 146, 263 (2001).
6. S. Veprek, A.S. Argon, Surf. Coat. Technol. 146–147, 175 (2001).
7. J. Musil, H. Polakova, Surf. Coat. Technol. 127, 99 (2000).
8. P. Kavrankova, H. D. Mannling, C. Eggs, S. Veprek, Surf. Coat. Technol. 146–147, 280 (2001).
9. P.K. Mayrhofer, F. Kunc, J. Musil, C. Mutterer, Thin Solid Films 415, 151 (2002).
10. P. Holubar, M. Jilek, M. Sima, Surf. Coat. Technol. 120–121, 184 (1999).
11. P. Kavrankova, M.G.J. Veprek-Heijman, M.F. Zawrah, S. Verpek, Thin Solid Films 467, 133 (2004).
12. J. Dorfel, W. Osterle, J. Urban, Surf. Coat. Technol. 111, 199 (1999).
13. V.Ch. Gonchikov, A.N. Tyumentsev, A.D. Korotaev, Yu.P. Pinzhin, Fizika metallov metallovedenie (rus) 63, 598 (1987).
14. P. Zeman, R. Cerstry, P.H. Mayrhofer, C. Mutterer, J. Musil, Mater. Sci. Engrs. A 289, 189 (2000).